Original Article | Neurointervention

eISSN 2005-8330
https://doi.org/10.3348/kjr.2023.0169
Korean J Radiol 2023;24(7):681-689

Korean Journal of Radiology
KJR

Reduction of Radiation Dose to Eye Lens in Cerebral 3D Rotational Angiography Using Head Off-Centering by Table Height Adjustment: A Prospective Study

Jae-Chan Ryu[1]*, Jong-Tae Yoon[2]*, Byung Jun Kim[3], Mi Hyeon Kim[2], Eun Ji Moon[1], Pae Sun Suh[1], Yun Hwa Roh[1], Hye Hyeon Moon[1], Boseong Kwon[1], Deok Hee Lee[1], Yunsun Song[1]

[1]Department of Radiology, Research Institute of Radiology, Asan Medical Center, University of Ulsan College of Medicine, Seoul, Korea
[2]Biomedical Engineering Research Center, Asan Institute for Life Sciences, Asan Medical Center, Seoul, Korea
[3]Advanced Therapies, Siemens Healthineers Ltd., Seoul, Korea

Objective: Three-dimensional rotational angiography (3D-RA) is increasingly used for the evaluation of intracranial aneurysms (IAs); however, radiation exposure to the lens is a concern. We investigated the effect of head off-centering by adjusting table height on the lens dose during 3D-RA and its feasibility in patient examination.

Materials and Methods: The effect of head off-centering during 3D-RA on the lens radiation dose at various table heights was investigated using a RANDO head phantom (Alderson Research Labs). We prospectively enrolled 20 patients (58.0 ± 9.4 years) with IAs who were scheduled to undergo bilateral 3D-RA. In all patients' 3D-RA, the lens dose-reduction protocol involving elevation of the examination table was applied to one internal carotid artery, and the conventional protocol was applied to the other. The lens dose was measured using photoluminescent glass dosimeters (GD-352M, AGC Techno Glass Co., LTD), and radiation dose metrics were compared between the two protocols. Image quality was quantitatively analyzed using source images for image noise, signal-to-noise ratio, and contrast-to-noise ratio. Additionally, three reviewers qualitatively assessed the image quality using a five-point Likert scale.

Results: The phantom study showed that the lens dose was reduced by an average of 38% per 1 cm increase in table height. In the patient study, the dose-reduction protocol (elevating the table height by an average of 2.3 cm) led to an 83% reduction in the median dose from 4.65 mGy to 0.79 mGy ($P < 0.001$). There were no significant differences between dose-reduction and conventional protocols in the kerma area product (7.34 vs. 7.40 Gy·cm^2, $P = 0.892$), air kerma (75.7 vs. 75.1 mGy, $P = 0.872$), and image quality.

Conclusion: The lens radiation dose was significantly affected by table height adjustment during 3D-RA. Intentional head off-centering by elevation of the table is a simple and effective way to reduce the lens dose in clinical practice.

Keywords: 3-dimensional rotational angiography; Lens radiation dose; Dose reduction; Head off-centering; Cerebral angiography

INTRODUCTION

Despite advancements in computed tomography (CT) and magnetic resonance angiography, cerebral angiography remains the gold standard imaging method for evaluating neurovascular diseases, including intracranial aneurysms. Alongside standard digital subtraction angiography, three-dimensional rotational angiography (3D-RA) is an indispensable tool that can accurately determine the size

Received: February 18, 2023 **Revised:** March 29, 2023 **Accepted:** April 24, 2023
*These authors contributed equally to this work.
Corresponding author: Yunsun Song, MD, PhD, Department of Radiology, Research Institute of Radiology, Asan Medical Center, University of Ulsan College of Medicine, 88 Olympic-ro 43-gil, Songpa-gu, Seoul 05505, Korea.
• E-mail: songsongggg@gmail.com

and shape of aneurysms, as well as their relationship with adjacent arteries [1-3]. However, 3D-RA entails additional radiation exposure and should, therefore, be used with caution [4,5].

Among the human organs, the eye is one of the most sensitive to radiation exposure, and the International Commission on Radiological Protection (ICRP) recommended limiting the radiation dose to the lens of the eye to reduce the risk of cataract [6]. However, as most aneurysms occur in the circle of Willis, the lens is inevitably exposed to radiation in 3D-RA. While many studies in the neurointerventional field have investigated different protocols for reducing radiation doses [7-15], few papers focused on dose reduction in 3D-RA, and none specifically focused on reducing the dose to the lens.

A phantom study in CT showed that head miscentering may be effective in reducing the radiation dose to the lens [16]. Accordingly, we hypothesized that the radiation dose in 3D-RA to the eye lens could also be reduced by intentionally off-centering the head by adjusting the imaging table height. We tested this hypothesis with a phantom model. assessing the feasibility of table height adjustment in reducing the dose to the lens during patient examination.

MATERIALS AND METHODS

Study Design

The basic concept of the lens dose reduction protocol was to reduce the lens' radiation exposure by increasing the patient table height during 3D-RA. The investigation comprised two parts: a phantom study and a patient study. The phantom study was first performed to verify our hypothesis that the table height would affect the lens' radiation dose and to determine the optimal table height. The patient study was conducted to determine the feasibility of the protocol in actual patients. To minimize the variables that can affect the radiation dose, each patient underwent the lens dose reduction protocol and the conventional protocol, which acted as a control.

Phantom Study

3D-RA was simulated with various table heights using a RANDO head phantom (Alderson Research Labs). The reference field-of-view (FOV) was set to the center of the head (0 cm). 3D-RA was performed once at every 1 cm change in table height between 4 cm above and 3 cm below the center of the head (Fig. 1A). The z-axis of the FOV was collimated to ≤ 7.5 cm in accordance with the routine patient examination. The lens' radiation dose was measured using three photoluminescent glass dosimeters (PLDs) on the right eye of the phantom.

Dosimetry System

The PLD reader system comprises a glass dosimeter (GD-352M, AGC Techno Glass Co., LTD) and an automatic reader unit (FGD-1000, AGC Techno Glass Co., LTD.) [17]. The glass dosimeter has a diameter of 1.5 mm and a length of 12 mm. The glass dosimeter holder (diameter, 4.33 mm; length, 14.52 mm) was made of acrylonitrile butadiene styrene resin. A tin filter compensated for the high response in low-energy photons. The automatic reader unit was used to read out the signal, and each PLD was read ten times as programmed by a dedicated software [18].

The lens dose was defined as the entrance skin dose directly measured by the PLD in the area closest to the lens. Three PLDs were used per lens, and the average value was used to estimate the dose applied to the lens. The PLDs were placed side-by-side in a thin fabric pouch and were oriented perpendicular to the z-axis to prevent inter-PLD interference. One pouch was used for each eye and they were attached to either side of goggles, made of thin, transparent films. The pouches were placed as close as possible to the lateral canthus of each eye at the same level as the lens on the lateral view (Fig. 2).

Radiation dose metrics were acquired using the onboard reference air kerma (mGy) and kerma area product (Gy·cm^2) meters. The values, which were displayed in the equipment's dose report, were also compared.

Patient Study

Among the patients who were scheduled to undergo cerebral angiography for the diagnosis and pre-treatment evaluation of known unruptured intracranial aneurysms at Asan Medical Center between June 2022 and July 2022, we prospectively enrolled those scheduled for 3D-RAs of both internal carotid arteries (ICAs) due to suspicion of bilateral or an anterior communicating artery (ACoA) aneurysm. The exclusion criteria were as follows: 1) age ≤ 18 or > 80 years, 2) any unexpected vascular lesion that required an additional angiogram, 3) intracranial materials including intracranial coils, clips, or embolic substances, and 4) refusal to participate. The ethics committee of Asan Medical Center approved this study (IRB No. 2022-0557), and informed consent was received from all patients (Fig. 3).

https://doi.org/10.3348/kjr.2023.0169

Korean Journal of Radiology
KJR

Routine cerebral angiography, which consisted of bilateral ICA and vertebral artery grams and 3D-RA for intracranial aneurysms was performed in all patients. When performing the ICA 3D examinations, the dose reduction protocol was randomly applied to one side, and the conventional protocol without table adjustment was applied to the other side as a control. In the conventional protocol, the FOV was located at the center of the head in the posteroanterior and lateral

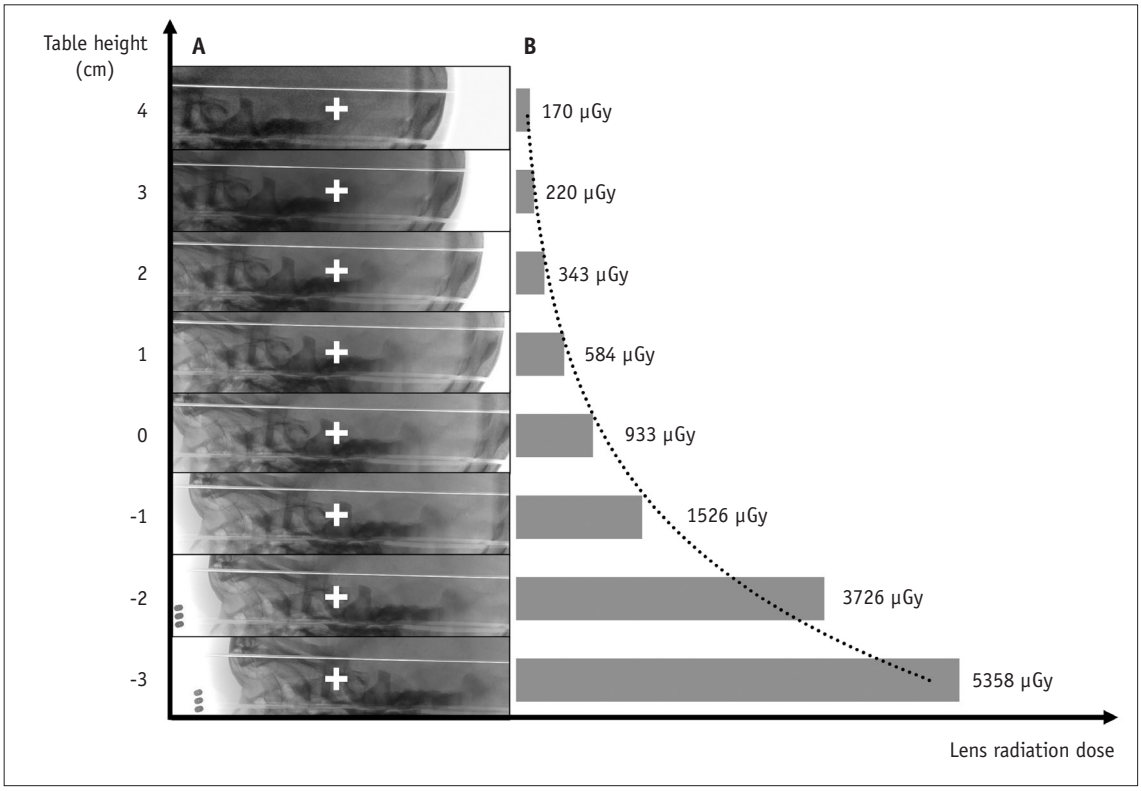

Fig. 1. Method of table height adjustment for evaluation of lens dose in the phantom study. **A:** The zero point (0 cm) of the table was determined when the center of the field-of-view (cross) was at the center of the head in the lateral projection during three-dimensional rotational angiography. The table height was changed from -3 cm to +4 cm. Three photoluminescent glass dosimeters (PLDs) on the right eye were shown in the lower table positions (-2 and -3 cm). **B:** Radiation doses measured by PLDs at each table height.

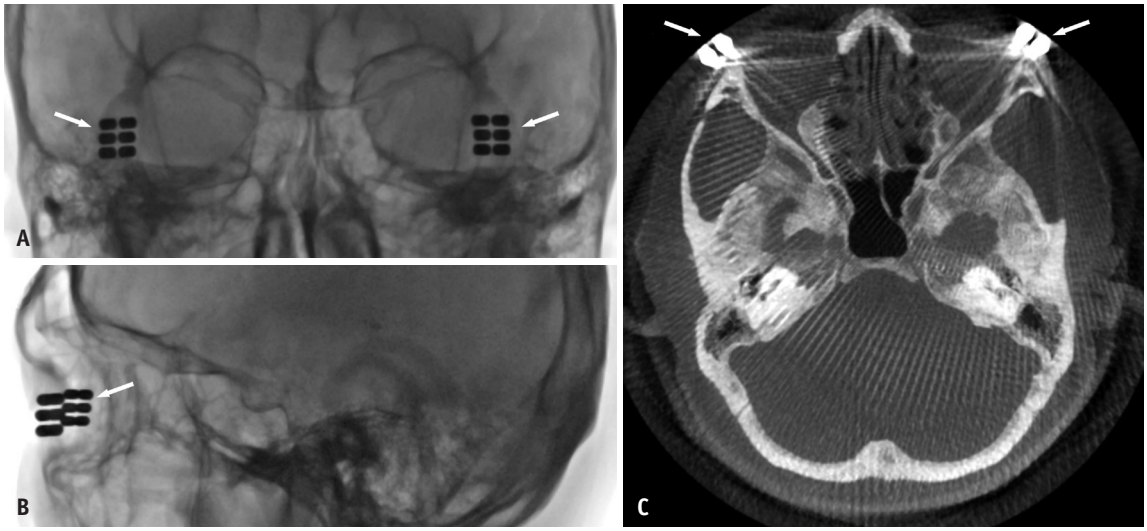

Fig. 2. The location of photoluminescent glass dosimeters (PLDs). The scout images of the frontal **(A)** and lateral **(B)** planes. **A, B:** A transparent goggles with three PLDs (arrows) in each pocket was used to estimate the radiation exposure to the eye lens. **C:** PLDs (arrows) are located on both lateral canthi on the axial image.

https://doi.org/10.3348/kjr.2023.0169

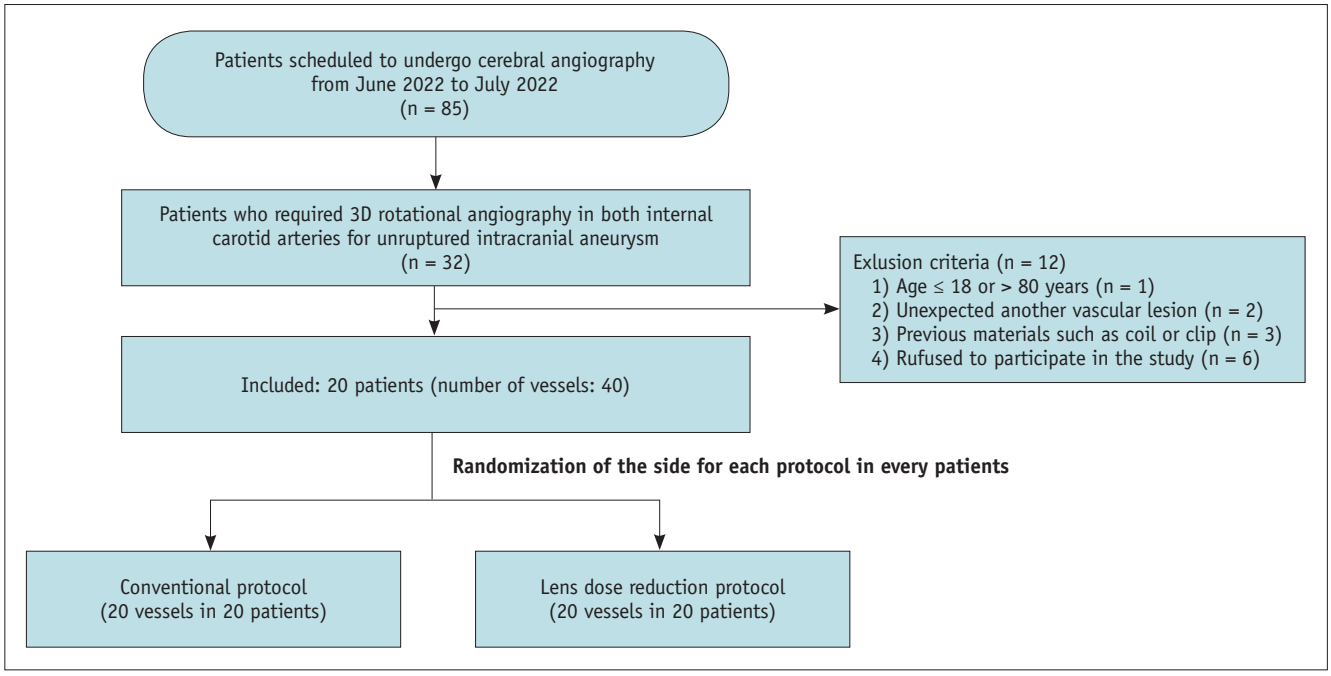

Fig. 3. Flow diagram of patients enrollment. According to the inclusion and exclusion criteria, a total of 20 patients were enrolled. 3D = three-dimensional

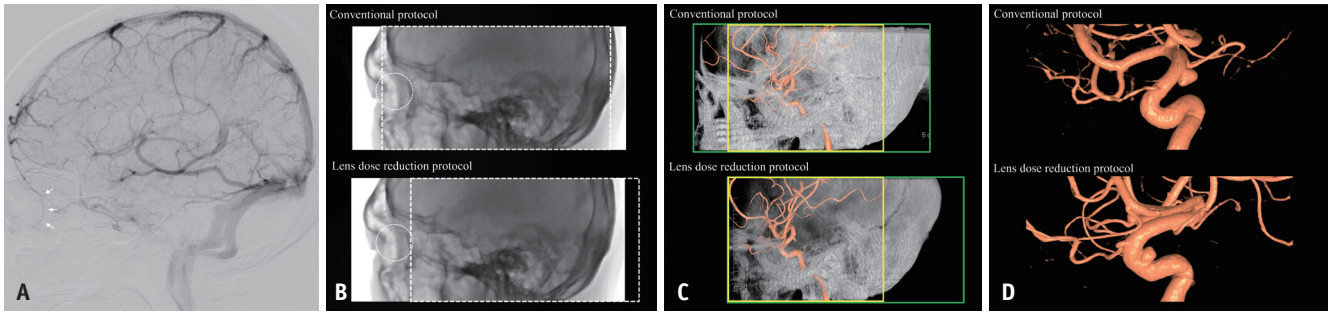

Fig. 4. Application of the lens dose reduction protocol. **A:** After two-dimensional internal carotid angiography, an imaginary circle was drawn along the choroidal blush (arrows) on the lateral view in order to represent the eyeball. **B:** On a native lateral view during the three-dimensional (3D) rotational angiography setting, the table height was adjusted until the anterior end of the field-of-view (FOV) was moved to just outside the circle, which was an increase in the table height of about 2 to 2.5 cm. **C:** The FOV of the first 3D reconstruction was indicated by a green square, and the second by a yellow square in both protocols. Note that the size and position of the FOV of the final 3D image are the same for both protocols. **D:** A representative case of intracranial aneurysms using the conventional protocol (upper) and dose reduction protocol (lower).

views so that all intracranial arteries were included. The size of the FOV in the z-axis direction was the same in both protocols. In the lens dose reduction protocol, the table was raised so that the anterior end of the FOV was located just behind the choroidal blush (Fig. 4). Except for the table height, other parameters, including the size of the FOV and image acquisition protocols, were the same in both ICA grams. The head size of the patient was measured in both anteroposterior and lateral directions on cross-sectional images at the lens level.

Imaging Equipment

All angiograms were obtained using a biplane angiography machine (Artis Zee; Siemens). All 3D-RA was acquired with digital subtraction angiography (DSA) mode (two 5-second rotations) (Supplementary Table 1). The kVp, milliampere (mA), pulse width, and copper filter were automatically determined by the angiographic system in the fixed routine protocol. Image protocols in these studies were the same as the optimized routine protocol used in our angiography suite. After 3D reconstruction, an interactive reconstruction with manually reduced FOV was followed in both protocols

https://doi.org/10.3348/kjr.2023.0169

Korean Journal of Radiology
KJR

to improve the spatial resolution of the reconstructed 3D images and solely include the area around the lesion of interest (Fig. 4).

Quantitative Image Analysis

For image quality assessment, axial 3D-RA source images were used to analyze the image noise, signal-to-noise ratio (SNR), and contrast-to-noise ratio (CNR). Image noise was determined as the standard deviation (SD) of the gray value by placing a region of interest (ROI; 1 cm^2) in the target aneurysm or adjacent parent artery (if the aneurysm is too small) to exclude any possibility of artifacts or image quality degradation that may occur as the target lesion shifts off-center while adjusting the height. The SNR was calculated by dividing the mean gray value of the target lesion by the image noise. The mean gray value and background noise were measured in the adjacent brain parenchyme. The CNR was calculated as the difference between the mean gray values of the target lesion and background, which was then divided by the background noise [19-21].

Qualitative Image Analysis

Three neuroradiologists (five years of experience each) independently assessed the image quality while blinded to the protocol used. A five-point Likert scale was used for image analysis: excellent (5-point: superior visualization of vasculature); good (4-point: good for visualization; small vessels also visible); fair (3-point: fair vessel visualization; distal parts of small arteries invisible but useful for diagnosis); poor (2-point: small arteries not discernible at all; larger arteries not sharply defined); fail (1-point: unsatisfactory for diagnosis).

Statistical Analysis

Continuous variables are expressed as mean ± SD or medians with interquartile ranges. Categorical variables are expressed as frequencies with percentages. The dose metrics in each protocol were compared using Student's paired *t*-test or Wilcoxon signed-rank test (if the assumption of normality is violated on the Shapiro–Wilk normality test). Pearson correlation tests were performed to determine the relationships between head size and radiation dose metrics. $P < 0.05$ was considered to denote statistical significance. Gwet's agreement coefficient with quadratic weight was used to calculate the inter-rater reliability for image quality evaluation. All statistical analyses were performed using R Statistical Software, version 4.1.0 (R Foundation for Statistical Computing).

RESULTS

Phantom Study

The radiation dose applied to the lens area decreased as the table height was increased (i.e., center of the FOV moving toward the back of the head) (Fig. 1B). The lens dose was the highest (5.36 mGy) when the table height was the lowest, which was 3 cm lower from the reference point (0 cm); the dose decreased by an average of 38% per 1-cm increase in the table height. The lens dose sharply increased by more than two-fold when the table was lowered by 2 cm from the reference point, which is when the PLDs were included on the lateral projection (Fig. 1A).

Patient Study

A total of 20 patients (female: 16 [80%], male: 4 [20%]) were included in the study, whose mean age was 58.0 ± 9.4 years (Table 1). Eleven patients had multiple aneurysms (total, n = 28 aneurysms). The locations of the cerebral aneurysms were as follows: distal ICA (16 aneurysms [43.3%]), ACoA (5 [13.5%]), anterior choroidal artery (5 [13.5%]), anterior cerebral artery (ACA) (4 [10.8%]), posterior communicating artery (3 [8.1%]), middle cerebral artery (2 [5.4%]), ophthalmic artery (1 [2.7%]), and

Table 1. Baseline Characteristics of the Study Patients

Variables	Values (n = 20)
Age, yr	58.0 ± 9.4
Sex, female	16 (80.0)
Patients with multiple aneurysms	11 (55.0)
Total number of aneurysms	37
Distal ICA	16 (43.3)
ACoA	5 (13.5)
AChA	5 (13.5)
ACA	4 (10.8)
PCoA	3 (8.1)
MCA	2 (5.4)
Ophthalmic artery	1 (2.7)
VA	1 (2.7)
Head size, mm	
Anteroposterior length	178.4 ± 7.5
Lateral length	154.0 ± 8.4

Data are presented as mean ± standard deviation or number (percentage) unless otherwise indicated. ICA = internal carotid artery, ACoA = anterior communicating artery, ACA = anterior cerebral artery, PCoA = posterior communicating artery, AChA = anterior choroidal artery, MCA = middle cerebral artery, VA = vertebral artery

 https://doi.org/10.3348/kjr.2023.0169

vertebral artery (1 [2.7%]).

On 3D examinations, the lens dose reduction protocol was applied to one ICA, and the conventional protocol was applied to the other ICA, and 11 (55%) patients had the lens dose reduction protocol applied on the right side. The table height was 2.3 cm higher on average on the side where the dose reduction protocol was applied. All target aneurysms were included in the FOV. The average radiation dose was 83% less on the dose reduction protocol side compared with the conventional protocol side (median of 0.79 vs. 4.65 mGy, $P < 0.001$) (Fig. 5). In both protocols, the doses measured in both eyes were not significantly different. In terms of overall radiation dose, there were no significant differences in the kerma area product (median of 7.34 vs. 7.40 Gy·cm^2, $P = 0.892$) and air kerma (mean of 75.7 vs. 75.1 mGy, $P = 0.872$) between the two protocols (Table 2).

On the conventional protocol side, the lens dose was significantly higher in patients with a smaller anteroposterior head length (R = -0.56, $P = 0.009$). In contrast, on the dose reduction protocol side, there was no significant difference in the dose according to the anteroposterior length (R = 0.04, $P = 0.873$) (Supplementary Fig. 1). The rate of dose reduction on the dose reduction protocol side was significantly greater in patients with a smaller anteroposterior length (R = -0.58, $P = 0.007$). In both protocols, the lateral length had a positive correlation with the anteroposterior length (R = 0.67, $P = 0.001$) and the lens dose.

In the quantitative analysis, the degree of image noise (mean 190.0 vs. 189.9, $P = 0.997$) was not significantly different between the two protocols. There were no significant differences in the SNR (mean 34.3 vs. 35.0, $P = 0.910$) and CNR (mean 90.5 vs. 79.8, $P = 0.350$) between the two protocols. In the qualitative analysis, image quality

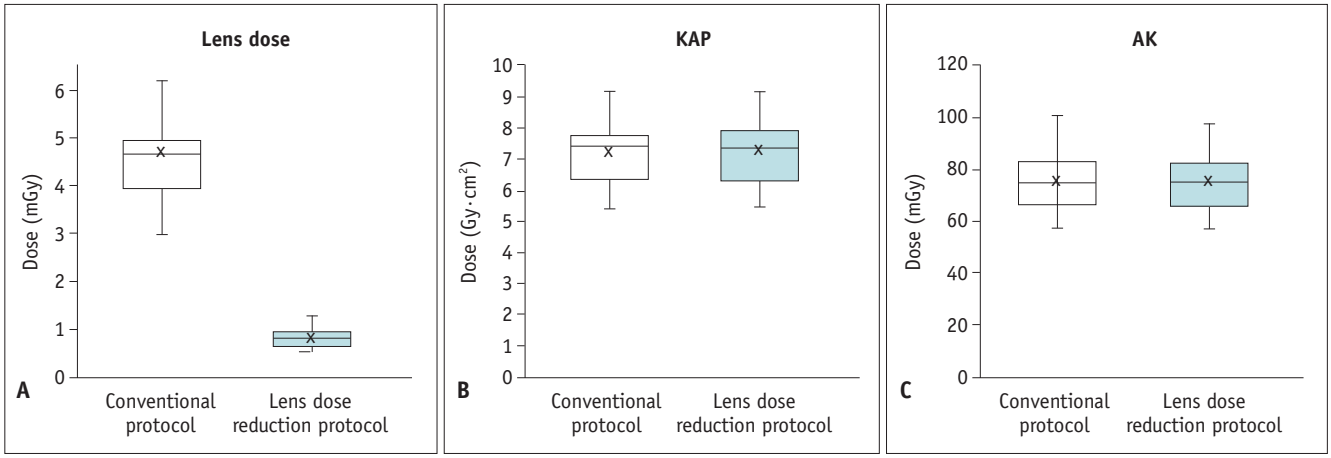

Fig. 5. The comparisons between conventional protocol and lens dose reduction protocol. **A-C**: Radiation doses measured to the eye lens, kerma area product (KAP), and air kerma (AK) values in the conventional protocol and the lens dose reduction protocol.

Table 2. Comparison of the Conventional Protocol versus the Dose Reduction Protocol in Terms of Radiation Dose and Image Quality

Variables	Conventional	Dose Reduction	*P*
Lens radiation dose, mGy	4.65 (3.99–4.94)	0.79 (0.63–0.91)	< 0.001
Right lens	4.64 ± 0.97	0.81 ± 0.27	< 0.001
Left lens	4.79 ± 1.86	0.79 ± 0.22	< 0.001
Kerma area product, Gy·cm^2	7.40 (6.40–7.69)	7.34 (6.35–7.89)	0.892
Air kerma, mGy	75.1 ± 11.9	75.7 ± 11.7	0.872
Quantitative image analysis			
Image noise	189.9 ± 84.1	190.0 ± 103.5	0.997
SNR	35.0 ± 17.1	34.3 ± 18.9	0.910
CNR	79.8 ± 28.5	90.5 ± 38.5	0.350
Qualitative image analysis	4.23 ± 0.49	4.23 ± 0.41	0.769

Data are presented as mean ± standard deviation or median (interquartile range) unless otherwise indicated. Continuous variables were compared using Student's *t*-test or Wilcoxon signed rank test according to the results of the Shapiro–Wilk normality test. SNR = signal-to-noise ratio, CNR = contrast-to-noise ratio

https://doi.org/10.3348/kjr.2023.0169

Korean Journal of Radiology
KJR

was not significantly different between the protocols (mean 4.23 vs. 4.23, $P = 0.769$). The inter-rater reliability was deemed satisfactory (0.62–0.65).

DISCUSSION

In our phantom study, we found that adjustment of the table height could significantly reduce the radiation exposure to the lens of the eye during 3D-RA, as the dose measured at the lens decreased by an average of 38% for every 1 cm increase in table height. Accordingly, the patient study showed that raising the table height by 2.3 cm, on average, led to an 83% reduction in lens radiation exposure without affecting the image quality. We also found that subjects with smaller head sizes had a higher lens dose, and the lens dose reduction protocol was more effective in these subjects.

In 2011, based on recent epidemiological studies, the ICRP revised the absorbed dose threshold for inducing cataracts to below 0.5 Gy, and the annual equivalent dose limit for occupational lens exposure from 150 mSv to 20 mSv, averaged over five consecutive years, with no single year exceeding 50 mSv [6]. The equivalent dose measured in the lens for cerebral angiography ranged from 5.5 to 12 mSv in previous phantom and clinical studies [4,22,23]. In our study, the mean absorbed dose in the lens during 3D-RA with two rotations was 4.7 mGy, which decreased to 0.8 mGy with the lens dose reduction protocol. While the dose for the 3D-RA alone did not reach the established threshold, it may hold significance when considering two-dimensional DSA, subsequent endovascular treatments, or follow-up angiography, which necessitate considerably higher radiation levels [23]. Moreover, lens opacity could manifest at dose levels below the current threshold, and given the uncertainties surrounding the dose threshold, it is essential to make continuous efforts to minimize the radiation dose applied to the lens [24].

The conventional low-dose protocols have primarily focused on reducing overall radiation exposure by lowering the detector entrance dose [7-9,25], while the lens dose reduction protocol aims to selectively decrease lens exposure without significantly altering the overall beam quality. The reduction in lens dose via table height adjustment is likely due to several mechanisms. First, when the tube is located laterally or on the anterior oblique aspect during 3D-RA, the lens is directly exposed to radiation without attenuation by the head. However, if the lens is excluded from the lateral FOV by increasing the table height, the dose is drastically reduced. The same mechanism may explain why the lens dose was higher in patients with smaller head sizes, where the lens is more likely to be included in the FOV on lateral tube position. Second, when the table is elevated, the number of frames that include the lens can be reduced.

Previous studies reported the effects of off-centering in CT in terms of radiation dose and noise [16,26,27]. When the center was lowered, the upper part of the patient became further away from the center and received a lower dose. On the other hand, the imaging noise increased as the target area moved away from the center, caused by the bow tie filter of the CT [16,27]. However, 3D-RA uses a flat-panel detector that does not employ such a filter; therefore, the noise would not be an issue as long as the radiation dose from the tube, which is estimated as the air kerma value, remains constant.

There are some potential issues when applying the lens dose reduction protocol. First, by raising the table, the far distal branch of the ACA may not be included in the 3D image because approximately 2 cm of the anterior aspect of the head is no longer included in the FOV. Therefore, this protocol cannot be applied when a lesion is suspected in that area. Second, if the empty space behind the head is included in the FOV while raising the table, the average attenuation of the FOV may decrease. Therefore, the radiation dose can be reduced by automatic exposure control, which can potentially affect image quality. Such an effect may be avoided by locating the Measuring Field in the center, and there was no significant difference in the kerma area product and air kerma values between the two groups in our study.

A simpler and more fundamental way to reduce the lens dose in 3D-RA would be to enable collimation in the x- and y-axes; however, in most angiographic machines, collimation is only available on one axis (top-bottom) in 3D-RA due to the truncation artifact. Although the latest angiographic machine enables partial left-right collimation in cone-beam CT acquisition, truncation artifacts might still be seen with overly narrow collimation in this axis. Lens dose reduction may be easily attained if this collimation could be performed without severe artifacts. Another way to reduce lens dose by decreasing FOV would be to use zoom. Although this method can simply reduce the FOV, the radiation dose (air kerma) can increase in proportion to the zoom factor, and the net effect on the lens dose has not been investigated.

Our study has some limitations. First, the lens dose measured in both the phantom and patient studies may not fully represent the actual lens dose as the measurements had to be taken at the lateral canthus of both eyes, closest to

 https://doi.org/10.3348/kjr.2023.0169

the lens, rather than the actual position of the lens. Second, the lens dose measurement was performed only during 3D-RA because the number of PLDs and frequent PLD replacement could interfere with the examination. Therefore, it was not possible to evaluate how much the protocol affected the total dose of cerebral angiography.

In conclusion, our phantom study demonstrated that the lens' radiation dose decreased as the table height increased during 3D-RA. Furthermore, our patient study showed that lens dose reduction by intentional head off-centering was feasible in clinical practice as the lens dose was reduced by 83% with a slight table elevation without affecting the image quality. This approach can be particularly beneficial for patients who require serial DSA examinations, where lens radiation exposure is inevitable.

Supplement

The Supplement is available with this article at https://doi.org/10.3348/kjr.2023.0169.

Availability of Data and Material

The dataset generated or analyzed during the study are available from the corresponding author on reasonable request.

Conflicts of Interest

The authors have no potential conflicts of interest to disclose.

Author Contributions

Conceptualization: Jae-Chan Ryu, Jong-Tae Yoon, Deok Hee Lee, Yunsun Song. Data curation: Jae-Chan Ryu, Jong-Tae Yoon, Yunsun Song. Formal analysis: Jae-Chan Ryu, Jong-Tae Yoon. Investigation: Jae-Chan Ryu, Jong-Tae Yoon, Byung Jun Kim, Mi Hyeon Kim, Eun Ji Moon, Boseong Kwon, Yunsun Song. Methodology: Jae-Chan Ryu, Jong-Tae Yoon, Deok Hee Lee, Yunsun Song. Supervision: Yunsun Song. Visualization: Jae-Chan Ryu, Jong-Tae Yoon, Yunsun Song. Writing—original draft: Jae-Chan Ryu, Jong-Tae Yoon, Yunsun Song. Writing—review & editing: all authors.

ORCID iDs

Jae-Chan Ryu
https://orcid.org/0000-0002-0935-963X
Jong-Tae Yoon
https://orcid.org/0000-0002-4332-7084
Byung Jun Kim
https://orcid.org/0000-0003-1720-1012
Mi Hyeon Kim
https://orcid.org/0000-0002-9232-0401
Eun Ji Moon
https://orcid.org/0000-0002-7687-3401
Pae Sun Suh
https://orcid.org/0000-0002-8618-9558
Yun Hwa Roh
https://orcid.org/0000-0002-8041-1621
Hye Hyeon Moon
https://orcid.org/0000-0001-8484-3117
Boseong Kwon
https://orcid.org/0000-0002-6113-9730
Deok Hee Lee
https://orcid.org/0000-0003-0355-0449
Yunsun Song
https://orcid.org/0000-0003-4738-0533

Funding Statement

None

REFERENCES

1. Abe T, Hirohata M, Tanaka N, Uchiyama Y, Kojima K, Fujimoto K, et al. Clinical benefits of rotational 3D angiography in endovascular treatment of ruptured cerebral aneurysm. *AJNR Am J Neuroradiol* 2002;23:686-688
2. Anxionnat R, Bracard S, Ducrocq X, Trousset Y, Launay L, Kerrien E, et al. Intracranial aneurysms: clinical value of 3D digital subtraction angiography in the therapeutic decision and endovascular treatment. *Radiology* 2001;218:799-808
3. van Rooij WJ, Sprengers ME, de Gast AN, Peluso JP, Sluzewski M. 3D rotational angiography: the new gold standard in the detection of additional intracranial aneurysms. *AJNR Am J Neuroradiol* 2008;29:976-979
4. Guberina N, Lechel U, Forsting M, Mönninghoff C, Dietrich U, Ringelstein A. Dose comparison of classical 2-plane DSA and 3D rotational angiography for the assessment of intracranial aneurysms. *Neuroradiology* 2016;58:673-678
5. Schueler BA, Kallmes DF, Cloft HJ. 3D cerebral angiography: radiation dose comparison with digital subtraction angiography. *AJNR Am J Neuroradiol* 2005;26:1898-1901
6. Stewart FA, Akleyev AV, Hauer-Jensen M, Hendry JH, Kleiman NJ, Macvittie TJ, et al. ICRP publication 118: ICRP statement on tissue reactions and early and late effects of radiation in normal tissues and organs--threshold doses for tissue reactions in a radiation protection context. *Ann ICRP* 2012;41:1-322
7. Ki HJ, Kim BS, Kim JK, Choi JH, Shin YS, Choi Y, et al. Low-dose 3D rotational angiography in measuring the size of intracranial aneurysm: in vitro feasibility study using

aneurysm phantom. *Neurointervention* 2021;16:59-63
8. Ki HJ, Kim BS, Kim JK, Choi JH, Shin YS, Choi Y, et al. Low-dose three-dimensional rotational angiography for evaluating intracranial aneurysms: analysis of image quality and radiation dose. *Korean J Radiol* 2022;23:256-263
9. Pearl MS, Torok C, Katz Z, Messina SA, Blasco J, Tamargo RJ, et al. Diagnostic quality and accuracy of low dose 3D-DSA protocols in the evaluation of intracranial aneurysms. *J Neurointerv Surg* 2015;7:386-390
10. Schneider T, Wyse E, Pearl MS. Analysis of radiation doses incurred during diagnostic cerebral angiography after the implementation of dose reduction strategies. *J Neurointerv Surg* 2017;9:384-388
11. Kim DJ, Park MK, Jung DE, Kang JH, Kim BM. Radiation dose reduction without compromise to image quality by alterations of filtration and focal spot size in cerebral angiography. *Korean J Radiol* 2017;18:722-728
12. Pearl MS, Torok C, Wang J, Wyse E, Mahesh M, Gailloud P. Practical techniques for reducing radiation exposure during cerebral angiography procedures. *J Neurointerv Surg* 2015;7:141-145
13. Söderman M, Holmin S, Andersson T, Palmgren C, Babic D, Hoornaert B. Image noise reduction algorithm for digital subtraction angiography: clinical results. *Radiology* 2013;269:553-560
14. Song Y, Han S, Kim BJ, Oh SH, Kim JS, Kim TI, et al. Low-dose fluoroscopy protocol for diagnostic cerebral angiography. *Neurointervention* 2020;15:67-73
15. Song Y, Han S, Kim BJ, Oh SH, Kim JS, Kim TI, et al. Feasibility of low-dose digital subtraction angiography protocols for the endovascular treatment of intracranial dural arteriovenous fistulas. *Neuroradiology* 2021;63:267-273
16. Anam C, Fujibuchi T, Toyoda T, Sato N, Haryanto F, Widita R, et al. The impact of head miscentering on the eye lens dose in CT scanning: phantoms study. *J Phys: Conf Ser* 2019;1204:012022
17. Kim JS, Park BR, Yoo J, Ha WH, Jang S, Jang WI, et al. Measurement uncertainty analysis of radiophotoluminescent glass dosimeter reader system based on GD-352M for estimation of protection quantity. *Nucl Eng Technol* 2022;54:479-485
18. Oonsiri P, Kingkaew S, Vannavijit C, Suriyapee S. Investigation of the dosimetric characteristics of radiophotoluminescent glass dosimeter for high-energy photon beams. *J Radiat Res Appl Sci* 2019;12:65-71
19. Lee KB, Goo HW. Quantitative image quality and histogram-based evaluations of an iterative reconstruction algorithm at low-to-ultralow radiation dose levels: a phantom study in chest CT. *Korean J Radiol* 2018;19:119-129
20. Otgonbaatar C, Ryu JK, Shin J, Woo JY, Seo JW, Shim H, et al. Improvement in image quality and visibility of coronary arteries, stents, and valve structures on CT angiography by deep learning reconstruction. *Korean J Radiol* 2022;23:1044-1054
21. Tan S, Soulez G, Diez Martinez P, Larrivée S, Stevens LM, Goussard Y, et al. Coronary stent artifact reduction with an edge-enhancing reconstruction kernel - a prospective cross-sectional study with 256-slice CT. *PLoS One* 2016;11:e0154292
22. Guberina N, Dietrich U, Forsting M, Ringelstein A. Comparison of eye-lens doses imparted during interventional and non-interventional neuroimaging techniques for assessment of intracranial aneurysms. *J Neurointerv Surg* 2018;10:168-170
23. Sandborg M, Rossitti S, Pettersson H. Local skin and eye lens equivalent doses in interventional neuroradiology. *Eur Radiol* 2010;20:725-733
24. Bolch WE, Dietze G, Petoussi-Henss N, Zankl M. Dosimetric models of the eye and lens of the eye and their use in assessing dose coefficients for ocular exposures. *Ann ICRP* 2015;44(1 Suppl):91-111
25. Pearl MS, Torok CM, Messina SA, Radvany M, Rao SN, Ehtiati T, et al. Reducing radiation dose while maintaining diagnostic image quality of cerebral three-dimensional digital subtraction angiography: an in vivo study in swine. *J Neurointerv Surg* 2014;6:672-676
26. Shaffiq Said Rahmat SM, Abdul Karim MK, Che Isa IN, Abd Rahman MA, Noor NM, Hoong NK. Effect of miscentering and low-dose protocols on contrast resolution in computed tomography head examination. *Comput Biol Med* 2020;123:103840
27. Habibzadeh MA, Ay MR, Asl AR, Ghadiri H, Zaidi H. Impact of miscentering on patient dose and image noise in x-ray CT imaging: phantom and clinical studies. *Phys Med* 2012;28:191-199